Journal of Statistical Physics, Vol. 55, Nos. 1/2, 1989

Quasiperiodicity and Randomness in Tilings of the Plane

C. Godrèche[1] and J. M. Luck[2,3,4]

Received August 2, 1988

We define new tilings of the plane with Robinson triangles, by means of generalized inflation rules, and study their Fourier spectrum. Penrose's matching rules are not obeyed; hence the tilings exhibit new local environments, such as three different bond lengths, as well as new patterns at all length scales. Several kinds of such generalized tilings are considered. A large class of deterministic tilings, including chiral tilings, is strictly quasiperiodic, with a tenfold rotationally symmetric Fourier spectrum. Random tilings, either locally (with extensive entropy) or globally random (without extensive entropy), exhibit a mixed (discrete + continuous) diffraction spectrum, implying a partial perfect long-range order.

KEY WORDS: Aperiodic tilings; inflation rules; quasiperiodicity.

1. INTRODUCTION

Studies of quasicrystalline structures have shown the importance of better understanding the concept of quasiperiodicity, in order to characterize the kind of order found in aperiodic matter (see, e.g., ref. 1). One may expect the existence of many types of order, between the perfect quasiperiodic tilings and the random ones, made of randomly packed units, with local pentagonal or icosahedral symmetry. Some recent work has been devoted to the role of defects in perfect quasiperiodic tilings.[2,3] More generally, it

[1] Service de Physique du Solide et de Résonance Magnétique, CEN Saclay, 91191 Gif-sur-Yvette Cedex, France.

[2] Service de Physique Théorique (Laboratoire de l'Institut de Recherche Fondamentale du Commissariat à l'Energie Atomique), CEN Saclay, 91191 Gif-sur-Yvette Cedex, France.

[3] University of Oxford, Department of Theoretical Physics, 1 Keble Road, Oxford OX1 3NP, Great Britain.

[4] University of Edinburgh, Department of Physics, The King's Buildings, Mayfield Road, Edinburgh EH9 3JZ, Great Britain.

0022-4715/89/0400-0001$06.00/0

is worthwhile investigating the extent to which quasiperiodicity is robust under changes of the tile ordering in a Penrose tiling. Other studies, concerned with random tilings,[4–10] proposed models of structure or growth for quasicrystals. Some of those structures exhibit narrow peaks in their Fourier transform (diffraction spectrum), implying approximate quasicrystalline order. The aim of both methods is to describe real quasicrystals, the structure of which probably lies between quasiperiodic (ideal) and random (amorphous).

The viewpoint we adopt here is intermediate between the above approaches. The tilings we study are generated by inflation rules, which may themselves be random. More precisely, we consider tilings made of Robinson triangles, which are particularly convenient when looking at inflation properties. We show that it is possible to tile the plane using self-similarity (inflation rules), without taking into account Penrose's matching rules. There are indeed several ways of cutting the Robinson triangles at each inflation step. We can consider three stages in a progressive disorganization of the perfect Penrose tiling: (1) the inflation rules are not the usual ones, but they are chosen once forever; (2) the inflation rules are chosen randomly at each generation, but they are the same for all triangles at a given step (global randomness); (3) the inflation rules are chosen randomly at each generation and for each triangle (local randomness). We study the Fourier spectrum of the structures thus obtained. In the first case, the Fourier spectrum is purely discrete, i.e., made of delta (Bragg) peaks, while in cases 2 and 3 it also contains a continuous part. Hence this study contributes to a better understanding of the questions raised above.

The present work may also be viewed as an extension of recent studies concerning one-dimensional models.[11–15] In ref. 15, we investigated the consequences of the absence of an average lattice, due to an unbounded density fluctuation, on the Fourier spectrum of a one-dimensional structure. We found a singular continuous spectrum, with nontrivial scaling behavior. This study mostly relied on the properties of an underlying substitution (inflation rule), which permits us to write recursion relations for the Fourier amplitudes of successive generations of the structure. Therefore, extending these ideas to the two-dimensional case, we were naturally led to consider the inflation properties of Penrose tilings, which are most easily described in terms of Robinson triangles.[16,17,18]

The setup of this article is as follows. In Section 2, taking the simple one-dimensional example of the Fibonacci chain, we recall how the Fourier spectrum of strictly self-similar structures can be studied, using only their inflation rules. Section 3 is devoted to a review of the construction of the Penrose tiling in terms of Robinson triangles, with a detailed description of the geometry of the inflation rules, which are then used to derive in an

alternative way the quasiperiodicity and tenfold symmetry of the Fourier spectrum of Penrose tilings. In Section 4, we define a new class of deterministic tilings, namely chiral tilings, and show that these are also quasiperiodic. Section 5 deals with (locally) random objects, the random Fibonacci chain and the random Penrose tiling. These new structures have an extensive structural entropy; their Fourier spectrum has a mixed nature (discrete + continuous), indicative of a partially perfect long-range order. In Section 6, further generalizations are proposed, including globally random tilings, which have a mixed spectrum, but no extensive entropy. A short discussion ends this last section.

2. A ONE-DIMENSIONAL EXAMPLE: THE FIBONACCI CHAIN

In this section, we illustrate by means of a simple example in one dimension the formalism that will be used later to study the Fourier transform of tilings of the plane. This approach, introduced by Bombieri and Taylor,[19] has already been used by the authors in a previous work with Aubry.[15]

The Fibonacci sequence is generated by the following substitution T, acting on two symbols, or "letters," 0 and 1:

$$T \begin{vmatrix} 0 \to 1 \\ 1 \to 10 \end{vmatrix} \tag{2.1}$$

Starting from the initial "word" $W_0 = 0$, we construct a sequence of words W_L by repeated action of T: $W_L = T(W_{L-1})$, and hence

$$W_L = T^L(0) \tag{2.2}$$

It can be easily shown that the form (2.1) of the substitution T yields the following concatenation rule:

$$W_L = W_{L-1} W_{L-2} \qquad (W_0 = 0;\ W_1 = 1) \tag{2.3}$$

Hence the words W_L converge to an infinite word W, called the Fibonacci sequence. From Eq. (2.3) it follows that W_L contains F_{L+1} letters, among which F_L are 1, and F_{L-1} are 0. Here and throughout the following, F_L denote the Fibonacci numbers, defined by the recursion

$$F_L = F_{L-1} + F_{L-2} \qquad (F_0 = 0;\ F_1 = 1) \tag{2.4}$$

These integers are related to the golden mean

$$\tau = \frac{\sqrt{5}+1}{2} \tag{2.5}$$

by the identities

$$F_L = \frac{1}{\sqrt{5}}\left[\tau^L - (-\tau^{-1})^L\right]$$
$$\tau^L = F_L \tau + F_{L-1} \tag{2.6}$$
$$(-\tau^{-1})^L = F_{L+1} - F_L \tau$$

The Fibonacci chain is built by putting atoms on a line, at abscissas u_n, in such a way that the bond lengths

$$l_n = u_n - u_{n-1} \qquad (u_0 = 0) \tag{2.7}$$

take two values, according to the Fibonacci sequence, namely $l_n = 1$ (short bond) if the nth letter of W is 0, and $l_n = 1 + \xi$ (long bond) if that nth letter is 1. Here, ξ is some additional parameter. The finite piece of the chain associated by such a construction to the word W_L has a length

$$\lambda_L = F_{L+1} + F_L \xi \tag{2.8}$$

Hence the mean interatomic distance (inverse density) reads

$$a = \lim_{L \to \infty} \frac{\lambda_L}{F_{L+1}} = 1 + \tau^{-1}\xi \tag{2.9}$$

It follows then from Eq. (2.6) that

$$\lambda_L = F_{L+1} a + (-\tau^{-1})^{L+1} \xi \tag{2.10}$$

Let now $g_L(q)$ denote the Fourier amplitude of the piece of the chain associated with W_L:

$$g_L(q) = \sum_{n=1}^{F_{L+1}} e^{-iqu_n} \tag{2.11}$$

The concatenation formula (2.3) then implies

$$g_L(q) = g_{L-1}(q) + e^{-iq\lambda_{L-1}} g_{L-2}(q) \tag{2.12}$$

The initial conditions of this recursion relation read $g_0(q) = e^{-iq}$; $g_1(q) = e^{-iq(1+\xi)}$. The local properties of the Fourier transform (diffraction spectrum) of the infinite structure are coded in the asymptotic growth of the amplitudes $g_L(q)$ for large L.[15,19] The largest possible growth is proportional to the sample size (number of atoms)

$$g_L(q) \underset{L \to \infty}{\approx} C F_{L+1} \tag{2.13}$$

The Fourier transform then has a delta peak at the value q of the wavevector, and the complex number C is the amplitude of that delta peak. It can be shown from Eq. (2.12) that the behavior (2.13) with nonvanishing C occurs only if $\lim_{L\to\infty} \exp(-iq\lambda_{L-1}) = 1$. By means of Eq. (2.10), this condition can be rewritten as $\lim_{L\to\infty} (qaF_L) = 0 \pmod{2\pi}$. The values of q which obey this last equality are given by

$$qa/2\pi = j + k\tau; \qquad (j, k) \text{ integers} \tag{2.14}$$

(see, e.g., ref. 15). The Fourier transform therefore contains delta peaks at a dense set of values of q, generated by the two incommensurate numbers 1 and τ, in units of $2\pi/a$. Note that the present method does not yield a closed expression for the amplitudes C of the delta peaks. Neither does it rule out, from a rigorous point of view, the presence of a continuous component in the Fourier spectrum. In the simple example of the Fibonacci chain, there are many other possible approaches to this question, like the projection method, which show that there is no continuous spectrum: the structure is strictly quasiperiodic. The present formalism will nevertheless be very useful in the following, in the study of cases where no other tool is at our disposal.

3. PENROSE TILING WITH ROBINSON TRIANGLES

3.1. Robinson Triangles

In this section, we first recall the description of the Penrose tiling in terms of Robinson triangles. These are particularly convenient to describe inflation rules, as explained below.

The Penrose tiling is usually described with two rhombs (or with darts and kites). If one cuts those polygons in a particular way, one obtains the two triangles P and Q of Fig. 1. These triangles have colored vertices, namely black and white ones. On Fig. 1 we only marked the black ones with a spot. Let us remark that there are actually two kinds of triangles P or Q, according to whether the marked vertices are to the right or to the left. More precisely, we denote by P^{R}, P^{L}, Q^{R}, Q^{L} the four different triangles (see Fig. 1).

The tiling is subject to the following two matching rules.[16,17,18]

1. Each edge of a triangle must be abutted by the edge of another triangle, in such a way that the colors of the vertices match.
2. In the case of a monochromatic edge (i.e., an edge joining two vertices of the same color), the smaller angle of one triangle

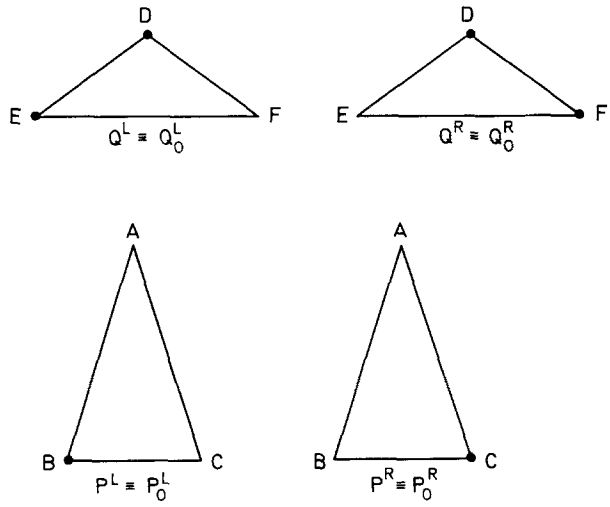

Fig. 1. Robinson triangles P_0 and Q_0.

must abut the smaller angle of the other one. This is equivalent to saying that each monochromatic edge is oriented: the monochromatic edges of adjacent tiles must have the same orientation.

The P and Q tiles can be composed to form new tiles (Fig. 2). Composing P and Q gives the triangle $\tau Q'$, which may be obtained by dilating Q by the factor τ and reversing its colors. The composition involves triangles of the same kind (R or L), and by convention the $\tau Q'$ triangle obtained is also of the same kind

$$P^R + Q^R \to \tau Q'^R; \qquad P^L + Q^L \to \tau Q'^L \tag{3.1}$$

This process of composition, or deflation, may be iterated (Fig. 3):

$$\tau Q'^L + P^R \to \tau P'^R; \qquad \tau Q'^R + P^L \to \tau P'^L \tag{3.2}$$

$$\tau P'^R + \tau Q'^R \to \tau^2 Q^R; \qquad \tau P'^L + \tau Q'^L \to \tau^2 Q^L \tag{3.3}$$

$$\tau^2 Q^L + \tau P'^R \to \tau^2 P^R; \qquad \tau^2 Q^R + \tau P'^L \to \tau^2 P^L \tag{3.4}$$

Note that Eqs. (3.3) and (3.4) are equivalent to Eqs. (3.1) and (3.2) up to an exchange of primed and nonprimed objects.

The above equations describe the composition of tiles, or deflation. The inflation process is the converse. It is equivalent to describing the process of inflation by starting with a larger triangle and cutting it. This point is illustrated by Fig. 2.

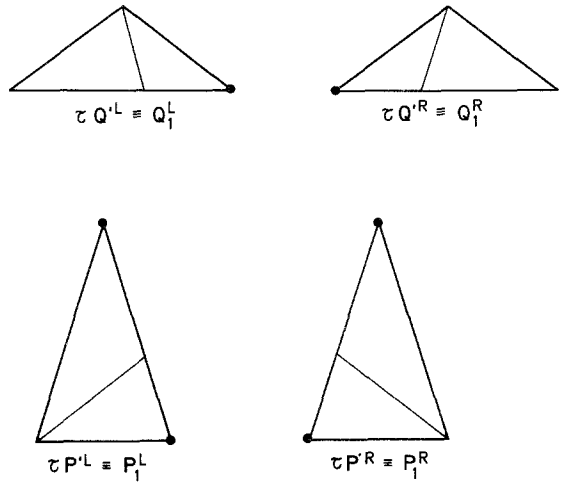

Fig. 2. First step of composition (deflation) for Robinson triangles, leading to P_1 and Q_1. Here P_0 and Q_0 are drawn with a smaller scale than that used in Fig. 1.

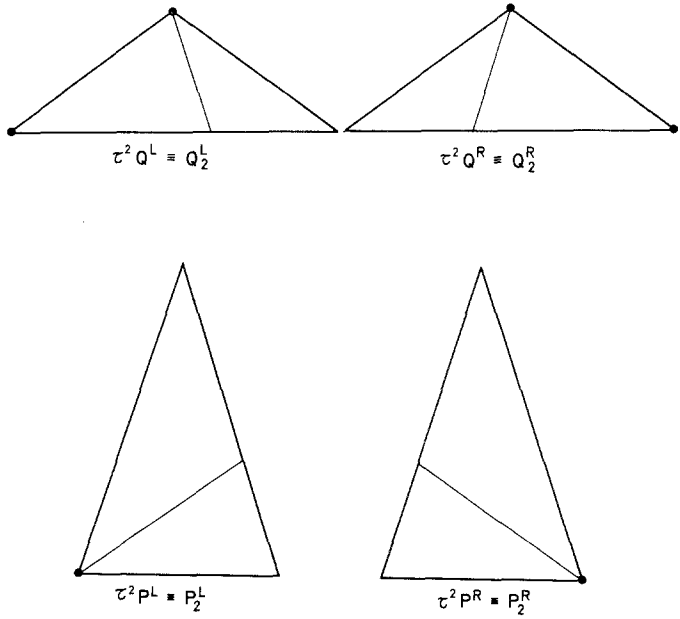

Fig. 3. Second step of composition of Robinson triangles leading to P_2 and Q_2.

In order to prepare the reader for the following sections, we need to introduce some notations which resemble those introduced in Section 2. Let us consider the tiles (elementary triangles) P and Q, which are the building blocks of the tiling, as the following "initial condition"

$$P^{\mathrm{R}} = P_0^{\mathrm{R}}; \qquad P^{\mathrm{L}} = P_0^{\mathrm{L}} \tag{3.5}$$

$$Q^{\mathrm{R}} = Q_0^{\mathrm{R}}; \qquad Q^{\mathrm{L}} = Q_0^{\mathrm{L}} \tag{3.6}$$

After one inflation step, one gets

$$\tau Q'^{\mathrm{R}} = Q_1^{\mathrm{R}} = T(Q^{\mathrm{R}}) \tag{3.7}$$

With these notations, Eq. (3.1) may be reexpressed as

$$Q_1^{\mathrm{R}} = P_0^{\mathrm{R}} Q_0^{\mathrm{R}}; \qquad Q_1^{\mathrm{L}} = P_0^{\mathrm{L}} Q_0^{\mathrm{L}} \tag{3.8}$$

Similarly, Eqs. (3.2)–(3.4) may be rewritten as

$$P_1^{\mathrm{R}} = P_0^{\mathrm{R}} Q_1^{\mathrm{L}} = P_0^{\mathrm{R}} P_0^{\mathrm{L}} Q_0^{\mathrm{L}}; \qquad P_1^{\mathrm{L}} = P_0^{\mathrm{L}} Q_1^{\mathrm{R}} = P_0^{\mathrm{L}} P_0^{\mathrm{R}} Q_0^{\mathrm{R}} \tag{3.9}$$

$$Q_2^{\mathrm{R}} = P_1^{\mathrm{R}} Q_1^{\mathrm{R}}; \qquad Q_2^{\mathrm{L}} = P_1^{\mathrm{L}} Q_1^{\mathrm{L}} \tag{3.10}$$

$$P_2^{\mathrm{R}} = P_1^{\mathrm{R}} Q_2^{\mathrm{L}} = P_1^{\mathrm{R}} P_1^{\mathrm{L}} Q_1^{\mathrm{L}}; \qquad P_2^{\mathrm{L}} = P_1^{\mathrm{L}} Q_2^{\mathrm{R}} = P_1^{\mathrm{L}} P_1^{\mathrm{R}} Q_1^{\mathrm{R}} \tag{3.11}$$

Unlike Eq. (2.3), which determined the structure in an unambiguous way by concatenation of one-dimensional words, Eqs. (3.8)–(3.11) just express an object counting, and need to be completed by geometrical information, as explained below.

Let us again notice that Eqs. (3.10) and (3.11) are equivalent to Eqs. (3.8) and (3.9) at the next inflation step. More generally, let us denote by P_n^{R}, P_n^{L},... the transforms of P^{R}, P^{L},... under n inflation steps,

$$P_n^{\mathrm{R}} = T(P_{n-1}^{\mathrm{R}}) = T^n(P_0^{\mathrm{R}}); \quad \text{etc.} \tag{3.12}$$

These objects obey the following recursion relations, which have the same meaning as Eqs. (3.8)–(3.11):

$$Q_n^{\mathrm{R}} = P_{n-1}^{\mathrm{R}} Q_{n-1}^{\mathrm{R}}; \qquad Q_n^{\mathrm{L}} = P_{n-1}^{\mathrm{L}} Q_{n-1}^{\mathrm{L}} \tag{3.13}$$

$$P_n^{\mathrm{R}} = P_{n-1}^{\mathrm{R}} Q_n^{\mathrm{L}} = P_{n-1}^{\mathrm{R}} P_{n-1}^{\mathrm{L}} Q_{n-1}^{\mathrm{L}}; \quad P_n^{\mathrm{L}} = P_{n-1}^{\mathrm{L}} Q_{n-1}^{\mathrm{R}} = P_{n-1}^{\mathrm{L}} P_{n-1}^{\mathrm{R}} Q_{n-1}^{\mathrm{R}} \tag{3.14}$$

Let us now give some quantitative characteristics of these objects. The triangles P_n and Q_n (either right or left) are τ^n times larger than the basic triangles P_0, Q_0. Their contents in tiles are described in a systematic way by the substitution matrix M_4, defined as follows. Let v_1, v_2, v_3, v_4 denote

the numbers of tiles of each type: P^{R}, P^{L}, Q^{R}, Q^{L}, in any finite piece A of the tiling. The numbers v_1', v_2', v_3', v_4' of tiles in the transformed object $T(A)$ under one step of inflation are given by

$$\begin{pmatrix} v_1' \\ v_2' \\ v_3' \\ v_4' \end{pmatrix} = M_4 \begin{pmatrix} v_1 \\ v_2 \\ v_3 \\ v_4 \end{pmatrix}; \qquad M_4 = \begin{pmatrix} 1 & 1 & 0 & 1 \\ 1 & 1 & 1 & 0 \\ 1 & 0 & 1 & 0 \\ 0 & 1 & 0 & 1 \end{pmatrix} \tag{3.15}$$

The eigenvalues of this matrix are τ^2, τ^{-2}, and $e^{\pm i\pi/3}$. The last two numbers are sixth roots of unity, hence the entries of M_4^n have oscillatory contributions, with period 6 in n. A straightforward calculation yields

$$M_4^n = \frac{1}{2} \begin{pmatrix} F_{2n+1} - \varepsilon_{n+2} & F_{2n+1} + \varepsilon_{n+2} & F_{2n} + \varepsilon_n & F_{2n} - \varepsilon_n \\ F_{2n+1} + \varepsilon_{n+2} & F_{2n+1} - \varepsilon_{n+2} & F_{2n} - \varepsilon_n & F_{2n} + \varepsilon_n \\ F_{2n} - \varepsilon_n & F_{2n} + \varepsilon_n & F_{2n-1} - \varepsilon_{n+1} & F_{2n-1} + \varepsilon_{n+1} \\ F_{2n} + \varepsilon_n & F_{2n} - \varepsilon_n & F_{2n-1} + \varepsilon_{n+1} & F_{2n-1} - \varepsilon_{n+1} \end{pmatrix} \tag{3.16}$$

where ε_n depends on n modulo 6: $\varepsilon_{6m} = \varepsilon_{6m+3} = 0$; $\varepsilon_{6m+1} = \varepsilon_{6m+2} = -1$; $\varepsilon_{6m+4} = \varepsilon_{6m+5} = +1$. The interpretation of M_4^n is the following: its first column gives the numbers of tiles of each type in P_n^{R}, its second column in P_n^{L}, etc. Hence P_n (either R or L) contains F_{2n+2} tiles (F_{2n+1} copies of P_0, and F_{2n} copies of Q_0), while Q_n contains F_{2n+1} tiles (F_{2n} copies of P_0, and F_{2n-1} copies of Q_0). The difference between numbers of P_0^{R} and P_0^{L}, or Q_0^{R} and Q_0^{L}, in any P_n or Q_n, is bounded by one in absolute value. Figure 4 shows the triangle P_6^{R}, made of 377 tiles, namely 117 P_0^{R}, 116 P_0^{L}, 72 Q_0^{R}, and 72 Q_0^{L}.

3.2. Geometrical Description of Inflation Rules

Let us come back to Eq. (3.8), for instance. This equation expresses the numbers and types of objects generated by the inflation (composition) procedure, as explained above. We now describe the actual geometrical transformations (namely rotations and translations) needed to bring together the two initial triangles P_0^{R} and Q_0^{R} which build Q_1^{R}. By convention, the initial condition is given by putting P_0^{R} and Q_0^{R} with their leftmost vertex at the origin, and with their symmetry axis parallel to the y axis. We also define the unit vectors $(\hat{e}_k)$ $(0 \leqslant k \leqslant 4)$ so that the angle between $\hat{e}_k$ and the positive x axis is equal to $k \cdot 2\pi/5$ (Fig. 5). Let us denote the rotation

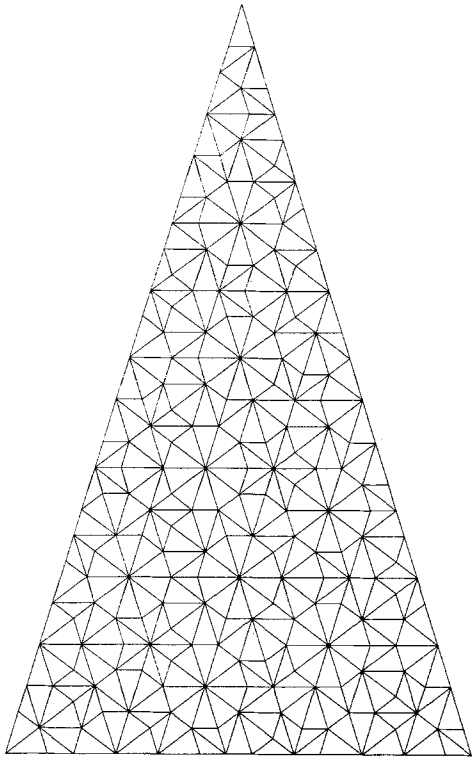

Fig. 4. Sixth iteration of the cutting procedure, yielding the triangle P_6^R.

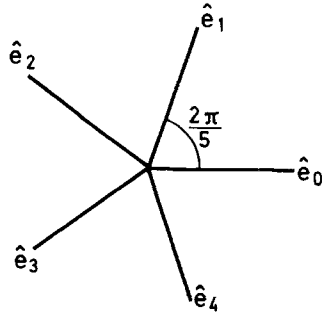

Fig. 5. Unit vectors in the plane of the tiling.

of angle $\theta = \pi/5$ in the plane by R, and the translation of vector $\mathbf{t}$ by $T(\mathbf{t})$, and use the condensed notation

$$[R^m, \mathbf{t}] \tag{3.17}$$

for the product of first the rotation R^m of angle $m\pi/5$ ($0 \leqslant m \leqslant 9$, since $R^{10} = R^0 = 1$), and then the translation $T(\mathbf{t})$.

With these notations, the complete geometrical version of the first part of Eq. (3.8) reads

$$Q_1^{\mathrm{R}} = [R^7, -\tau\hat{e}_3]\, P_0^{\mathrm{R}} + [R^6, -\tau\hat{e}_3]\, Q_0^{\mathrm{R}} \tag{3.18}$$

In an analogous way, the first equality in Eq. (3.13) becomes

$$Q_n^{\mathrm{R}} = [R^7, -\tau^n\hat{e}_3]\, P_{n-1}^{\mathrm{R}} + [R^6, -\tau^n\hat{e}_3]\, Q_{n-1}^{\mathrm{R}} \tag{3.19}$$

To summarize, let us give all the geometrical recursion relations needed hereafter:

$$Q_n^{\mathrm{R}} = [R^7, -\tau^n\hat{e}_3]\, P_{n-1}^{\mathrm{R}} + [R^6, -\tau^n\hat{e}_3]\, Q_{n-1}^{\mathrm{R}} \tag{3.20}$$

$$Q_n^{\mathrm{L}} = [R^3, \tau^n\hat{e}_0]\, P_{n-1}^{\mathrm{L}} + [R^4, \tau^{n+1}\hat{e}_0]\, Q_{n-1}^{\mathrm{L}} \tag{3.21}$$

$$P_n^{\mathrm{R}} = [R^7, \tau^{n-1}\hat{e}_1]\, P_{n-1}^{\mathrm{R}} + [R^3, \tau^n\hat{e}_0]\, Q_n^{\mathrm{L}} \tag{3.22}$$

$$P_n^{\mathrm{L}} = [R^3, \tau^n\hat{e}_0]\, P_{n-1}^{\mathrm{L}} + [R^7, \tau^{n+1}\hat{e}_1]\, Q_n^{\mathrm{R}} \tag{3.23}$$

The last two equations may be expanded in the following form:

$$P_n^{\mathrm{R}} = [R^7, \tau^{n-1}\hat{e}_1]\, P_{n-1}^{\mathrm{R}} + [R^6, \tau^n(\hat{e}_0 - \hat{e}_4)]\, P_{n-1}^{\mathrm{L}} + [R^7, \tau^{n+1}\hat{e}_1]\, Q_{n-1}^{\mathrm{L}} \tag{3.24}$$

$$P_n^{\mathrm{L}} = [R^3, \tau^n\hat{e}_0]\, P_{n-1}^{\mathrm{L}} + [R^4, -\tau^n\hat{e}_3]\, P_{n-1}^{\mathrm{R}} + [R^3, -\tau^n\hat{e}_3]\, Q_{n-1}^{\mathrm{R}} \tag{3.25}$$

using the elementary rule for products of rotations and translations

$$[R^m, \mathbf{t}] \circ [R^{m'}, \mathbf{t}'] = [R^{m+m'}, \mathbf{t} + R^m\mathbf{t}'] \tag{3.26}$$

3.3. Fourier Transform

We now use the above inflation rules to derive recursive relations between Fourier amplitudes, along the lines of Section 2. Let us first define what we mean by the Fourier transform of the tiling. To a particular kind of elementary triangle, e.g., the initial triangle P_0^{R}, we associate a mass distribution described by a function $\rho(\mathbf{x})$, where $\mathbf{x}$ denotes a point inside the triangle. For instance, ρ may be a uniform mass distribution inside the

triangle, or a delta function at the center of the triangle, or anything else. Thus, what we consider here is actually the dual of the tiling, since usually the atomic masses are located at the vertices. The Fourier transform of this function is defined as usual,

$$\mathcal{F}[\rho(\mathbf{x})] = G(\mathbf{q}) = \int \exp(-i\mathbf{q}\cdot\mathbf{x})\,\rho(\mathbf{x})\,d^2x \tag{3.27}$$

Under a rotation R, the distribution $\rho(\mathbf{x})$ becomes $\rho(R\mathbf{x})$, and the Fourier amplitude changes into

$$\mathcal{F}[\rho(R\mathbf{x})] = G(R^{-1}\mathbf{q}) \tag{3.28}$$

Similarly, under a translation $T(\mathbf{t})$, the distribution $\rho(\mathbf{x})$ becomes $\rho(\mathbf{x}+\mathbf{t})$, and the Fourier amplitude changes into

$$\mathcal{F}[\rho(\mathbf{x}+\mathbf{t})] = \exp(-i\mathbf{q}\cdot\mathbf{t})\,G(\mathbf{q}) \tag{3.29}$$

Using Eqs. (3.27)–(3.29), it is now possible to translate the geometrical recursion equations (3.20)–(3.25) into recursive equations for the associated Fourier amplitudes. One finds easily by the same type of arguments as in Section 2

$$\begin{aligned} P_n^{\mathrm{R}}(\mathbf{q}) &= \exp(-i\mathbf{q}\cdot\tau^{n-1}\hat{e}_1)\,P_{n-1}^{\mathrm{R}}(R^3\mathbf{q}) \\ &\quad + \exp[-i\mathbf{q}\cdot\tau^n(\hat{e}_0-\hat{e}_4)]\,P_{n-1}^{\mathrm{L}}(R^4\mathbf{q}) \\ &\quad + \exp(-i\mathbf{q}\cdot\tau^{n+1}\hat{e}_1)\,Q_{n-1}^{\mathrm{L}}(R^3\mathbf{q}) \end{aligned} \tag{3.30}$$

$$\begin{aligned} P_n^{\mathrm{L}}(\mathbf{q}) &= \exp(-i\mathbf{q}\cdot\tau^n\hat{e}_0)\,P_{n-1}^{\mathrm{L}}(R^7\mathbf{q}) \\ &\quad + \exp(i\mathbf{q}\cdot\tau^n\hat{e}_3)[P_{n-1}^{\mathrm{R}}(R^6\mathbf{q}) + Q_{n-1}^{R}(R^7\mathbf{q})] \end{aligned} \tag{3.31}$$

$$Q_n^{\mathrm{R}}(\mathbf{q}) = \exp(i\mathbf{q}\cdot\tau^n\hat{e}_3)[P_{n-1}^{\mathrm{R}}(R^3\mathbf{q}) + Q_{n-1}^{\mathrm{R}}(R^4\mathbf{q})] \tag{3.32}$$

$$\begin{aligned} Q_n^{\mathrm{L}}(\mathbf{q}) &= \exp(-i\mathbf{q}\cdot\tau^n\hat{e}_0)\,P_{n-1}^{\mathrm{L}}(R^7\mathbf{q}) \\ &\quad + \exp(-i\mathbf{q}\cdot\tau^{n+1}\hat{e}_0)\,Q_{n-1}^{\mathrm{L}}(R^6\mathbf{q}) \end{aligned} \tag{3.33}$$

Here $P_n^{\mathrm{R}}(\mathbf{q})$ stands for the Fourier amplitude associated with the object P_n^{R}, etc. The initial conditions of the recursion (3.30)–(3.33) depend on the actual form of the density $\rho(\mathbf{x})$ that we have put onto each type of elementary triangle.

We now discuss the implications of the recursion relations derived above, leaving the initial conditions $P_0^{\mathrm{R}}(\mathbf{q})$, etc., unspecified. Therefore our results hold for any mass distribution living on the four types of elementary triangles.

Just as we did in Section 2, let us consider the wavevectors $\mathbf{q}$ corresponding to the largest possible growth of the Fourier amplitudes, which is proportional to the sample size (number of tiles). In analogy with the one-dimensional case, it can be argued that this largest growth, corresponding to a delta peak, occurs generically if and only if all the phases entering Eqs. (3.30)–(3.33) vanish in the $n \to \infty$ limit. It can be checked that this condition is fulfilled for wavevectors of the form

$$\mathbf{q} = 4\pi \sum_{k=0}^{4} m_k \hat{e}_k \tag{3.34}$$

where the m_k are five integers, and the unit vectors $\hat{e}_k$ have been defined above. Indeed, since $2\cos(2\pi/5) = \tau^{-1}$ and $2\cos(4\pi/5) = -\tau$, we have

$$\mathbf{q} \cdot \hat{e}_0 = 2\pi[m_0 + \tau^{-1}(m_1 + m_4) - \tau(m_2 + m_3)]$$

Hence $\mathbf{q} \cdot \tau^n \hat{e}_0 / 2\pi$ can be shown, by means of Eq. (2.6), to converge to zero (mod 1). For $\mathbf{q}$ given by Eq. (3.34), Eqs. (3.30)–(3.33) involve, in the $n \to \infty$ limit, a constant asymptotic 40×40 matrix $\mathcal{M}_{40}$ with integer entries (there are four equations, which connect $\mathbf{q}$ to $R\mathbf{q}$,..., $R^9\mathbf{q}$). This matrix can be easily diagonalized by means of the superpositions

$$P^{\mathrm{R}}_{n,l} = \sum_{k=0}^{9} \omega^{kl} P^{\mathrm{R}}_n(R^k \mathbf{q}) \qquad (0 \leqslant l \leqslant 9) \tag{3.35}$$

and three analogous quantities for the other types of tiles, where $\omega = \exp(i\pi/5)$. Indeed the asymptotic matrix $\mathcal{M}_{40}$ is decomposed into ten 4×4 blocks $\mathcal{M}_{4,l}$

$$\mathcal{M}_{4,l} = \begin{pmatrix} \omega^{7l} & \omega^{6l} & 0 & \omega^{7l} \\ \omega^{4l} & \omega^{3l} & \omega^{3l} & 0 \\ \omega^{7l} & 0 & \omega^{6l} & 0 \\ 0 & \omega^{3l} & 0 & \omega^{4l} \end{pmatrix} \tag{3.36}$$

The eigenvalues of $\mathcal{M}_{4,l}$ read

$$\lambda = \tfrac{1}{2}[\mu \pm (\mu^2 - 4)^{1/2}] \tag{3.37}$$

with $\mu = c + c' \pm [(c - c')^2 + 1]^{1/2}$; $c = \cos(3l\pi/5)$ and $c' = \cos(4l\pi/5)$. Both $\pm$ symbols in the above equations are independent, so that λ assumes four values. If $l = 0$, the substitution matrix M_4 of Eq. (3.15) is recovered, with its leading eigenvalue τ^2. The next largest eigenvalues are $\pm\tau$, which occur for all odd values of l. The original Fourier amplitudes are given by

$$P^{\mathrm{R}}_n(R^k \mathbf{q}) = \sum_{l=0}^{9} \omega^{-kl} P^{\mathrm{R}}_{n,l} \qquad (0 \leqslant k \leqslant 9) \tag{3.38}$$

The $l=0$ term grows as τ^{2n} and yields a delta peak with a k-independent amplitude. Thus, the well-known tenfold symmetry of the Fourier spectrum is restored in the limit of a large system, even if the microscopic mass distribution $\rho(\mathbf{x})$ has no special symmetry property. With the same caveats as for the Fibonacci chain, the present approach has shown that the Penrose tiling made of Robinson triangles has a quasiperiodic Fourier transform, consisting of delta peaks at the wavevectors given by Eq. (3.34), with tenfold rotational symmetry.

The usually defined Penrose lattice, with atoms at its vertices, has a denser Fourier spectrum, with delta peaks for

$$\mathbf{q} = 2\pi \sum_{k=0}^{4} m_k \hat{e}_k \tag{3.39}$$

The factor of 2 between both results is by no means a mistake, since putting atoms at vertices cannot be viewed as a limiting case of our model, which puts mass onto the basic triangles, because the coordination number is not a constant. Let us mention for sake of completeness that, for values of $\mathbf{q}$ given by Eq. (3.39) which are not of the form (3.34) (i.e., when the m_k are not all of the same parity), the asymptotic form of Eqs. (3.30)–(3.33) involves signs (± 1), which have period 3 in n. Hence the analogous of $\mathcal{M}_{40}$ is now the product of three consecutive such matrices. The largest eigenvalue of this product is always equal to $\lambda = 4.188082$. Hence, for all those values of $\mathbf{q}$, the Fourier amplitudes only grow like N^{γ}, where $N \sim \tau^{2n}$ is the number of tiles in the sample, and $\gamma = (\ln \lambda)/(6 \ln \tau) = 0.496054$. The exponent γ is smaller than 1, as expected: there are no delta peaks at those points.

4. GENERALIZED INFLATION RULES: CHIRAL TILINGS

One may wonder what happens if one completely relaxes the matching rules, composing the tiles P and Q in any order, just as in a random growth process. It is well known that only a vanishingly small fraction of such arrangements of tiles will lead to a tiling. Hence, we will restrict the possible arrangements by imposing inflation rules, allowing them to be more general than those described in Section 3 (which led to the Penrose tiling).

As mentioned above, the matching rules are equivalent to cutting rules. Therefore, in order to relax the matching rules, one may choose to violate the cutting rules. For instance, one may cut a triangle P^{R} as if it were a triangle P^{L}. This may be done for a Q triangle as well. Let us notice that this alteration changes the numbers of right or left triangles of each

kind (P or Q), but of course not the total numbers of P or Q. Therefore the concentrations of P and Q triangles are the same as in the Penrose tiling.

As mentioned in the introduction, several cases may be considered. Let us first study chiral tilings.

The right chiral tiling is obtained by cutting repeatedly all Robinson triangles as right triangles. The superscript R is omitted from now on. Of course, the left chiral tiling is defined in an analogous way. Let P_n and Q_n denote the nth iterates of that inflation procedure, starting respectively from P_0 and Q_0. The recursion relations which express the tile contents of the triangles, in analogy with Eqs. (3.13) and (3.14), read

$$P_n = P_{n-1}^2 Q_{n-1}; \qquad Q_n = P_{n-1} Q_{n-1} \tag{4.1}$$

The associated substitution matrix

$$M_2 = \begin{pmatrix} 2 & 1 \\ 1 & 1 \end{pmatrix} \tag{4.2}$$

has eigenvalues τ^2 and τ^{-2}, and its nth power is

$$M_2^n = \begin{pmatrix} F_{2n+1} & F_{2n} \\ F_{2n} & F_{2n-1} \end{pmatrix} \tag{4.3}$$

The numbers of tiles P_0 and Q_0 at each generation are therefore the same as for the Penrose tiling. Figure 6 shows the sixth iterate P_6, to be compared with Fig. 4. The triangle P_6 also contains 377 tiles, namely 233 P_0 and 144 Q_0. There are several new local patterns and vertex environments, which are not present in the Penrose tiling. In particular, there exist vertices with coordination number $z = 3$. Moreover, the bond lengths assume three different values, in ratio $1 : \tau : \tau^2$, whereas only two different kinds of bonds $(1 : \tau)$ are met in usual Penrose tilings.

The Fourier amplitudes, still denoted $P_n(\mathbf{q})$, $Q_n(\mathbf{q})$, can be evaluated along the lines of Section 3. There are now only two coupled equations,

$$\begin{aligned} P_n(\mathbf{q}) = {} & \exp(-i\mathbf{q} \cdot \tau^{n-1} \hat{e}_1)\, P_{n-1}(R^3\mathbf{q}) \\ & + \exp[-i\mathbf{q} \cdot \tau^n (\hat{e}_0 - \hat{e}_4)]\, P_{n-1}(R^4\mathbf{q}) \\ & + \exp(-i\mathbf{q} \cdot \tau^{n+1} \hat{e}_1)\, Q_{n-1}(R^3\mathbf{q}) \end{aligned} \tag{4.4}$$

$$Q_n(\mathbf{q}) = \exp(i\mathbf{q} \cdot \tau^n \hat{e}_3)[P_{n-1}(R^3\mathbf{q}) + Q_{n-1}(R^4\mathbf{q})] \tag{4.5}$$

Leaving the initial conditions unspecified, we can still argue that there is a delta peak at each value of $\mathbf{q}$ such that all phases entering Eqs. (4.4) and

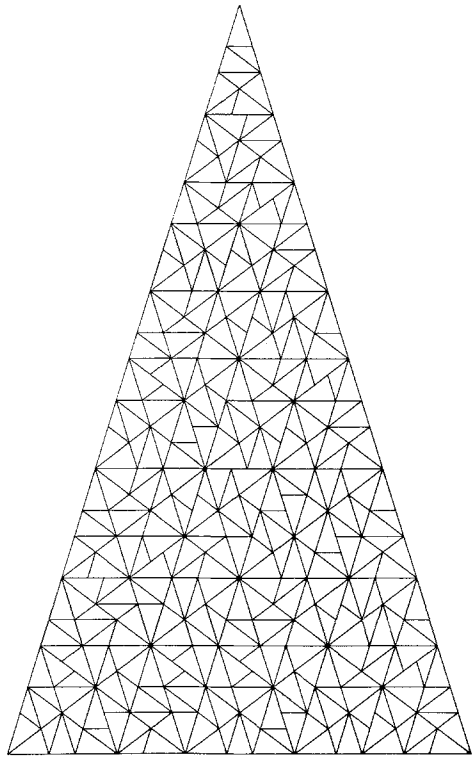

Fig. 6. A (right) chiral tiling after six steps of the cutting procedure.

(4.5) go to zero. This condition is obeyed for the set of wavevectors given by Eq. (3.34). For those values of $\mathbf{q}$, Eqs. (4.4) and (4.5) involve a constant asymptotic 20×20 matrix $\mathscr{M}_{20}$, which can be decomposed into ten 2×2 blocks $\mathscr{M}_{2,l}$ $(0 \leqslant l \leqslant 9)$,

$$\mathscr{M}_{2,l} = \begin{pmatrix} \omega^{6l} + \omega^{7l} & \omega^{7l} \\ \omega^{7l} & \omega^{6l} \end{pmatrix} \tag{4.6}$$

by a change of variables analogous to Eq. (3.35). The eigenvalues of these blocks are

$$\lambda = \tfrac{1}{2}(2\omega^{6l} + \omega^{7l} \pm \omega^{2l}\sqrt{5}) \tag{4.7}$$

As expected, $l = 0$ gives back the matrix M_2 of Eq. (4.2). Its leading eigenvalue τ^2 is responsible for the existence of delta peaks at all the values of $\mathbf{q}$ given by Eq. (3.34), and for the restoration of the tenfold symmetry of the diffraction pattern. The next largest eigenvalues occur for $l = 1$ and 9; they

are complex conjugate, with modulus $\rho = 2.497212$. Hence, beyond their leading behavior ($\sim N \sim \tau^{2n}$), the Fourier amplitudes P_n and Q_n have oscillatory subleading contributions ($\sim \rho^n$). The relative weight of these terms is of the order of

$$\left(\frac{\rho}{\tau^2}\right)^n \sim N^{-\Delta}, \qquad \text{with} \quad \Delta = 1 - \frac{\ln \rho}{2 \ln \tau} = 0.049093 \tag{4.8}$$

This small value of the correction exponent Δ implies a very slow and non-monotonous convergence of Fourier amplitudes. This is indeed one of the major differences between the chiral tilings under consideration and the Penrose tiling, where Fourier amplitudes have smooth $N^{-1/2}$ corrections that can be interpreted as a boundary (perimeter) effect.

5. GENERALIZED INFLATION RULES: RANDOM TILINGS

5.1. The Random Fibonacci Chain

Just as we did in Section 2 for deterministic (nonrandom) structures, let us first illustrate our construction of random tilings, and study the nature of their Fourier transform, by considering a one-dimensional example, namely the random Fibonacci chain.

We first generate a random Fibonacci sequence by a stochastic version $\mathscr{T}$ of the substitution T defined in Section 2. $\mathscr{T}$ still acts on the two letters 0 and 1, according to the following random rule

$$\mathscr{T} \begin{cases} 0 \to 1 \\ 1 \to \begin{cases} 10 & (\text{with prob } p) \\ & \text{or} \\ 01 & (\text{with prob } r = 1 - p) \end{cases} \end{cases} \tag{5.1}$$

where p is some fixed probability ($0 \leqslant p \leqslant 1$). This random rule holds independently at each time that $\mathscr{T}$ acts on a 1. We define an infinite sequence of random words

$$\mathscr{W}_L = \mathscr{T}^L(0) \tag{5.2}$$

$\mathscr{W}_0 = 0$ and $\mathscr{W}_1 = 1$ are certain, i.e., they take only one possible value. $\mathscr{W}_2$ is either 10 or 01, with respective probabilities p and r. $\mathscr{W}_3$ is either 101, 011, or 110, with respective probabilities $p^2 + r^2$, pr, and pr, etc. $\mathscr{W}_L$ is just a random reshuffling of the F_{L+1} letters, among which F_L are 1 and F_{L-1} are 0, of its deterministic counterpart W_L, defined in Section 2.

The concatenation rule (2.3) has a stochastic analogue in the present case,

$$\mathscr{W}_L = \begin{cases} \mathscr{W}_{L-1}\mathscr{W}_{L-2} & \text{(with prob } p\text{)} \\ & \text{or} \\ \mathscr{W}_{L-2}\mathscr{W}_{L-1} & \text{(with prob } r\text{)} \end{cases} \tag{5.3}$$

with the convention that the three sources of randomness in the rhs, namely both words and their concatenation procedure, have to be considered as independent. The $\mathscr{W}_L$ converge (in distribution) to an infinite random word $\mathscr{W}$, the random Fibonacci sequence.

We determine now the structural entropy of this object. Let N_L denote the number of different realizations of $\mathscr{W}_L$. We have seen before that $N_0 = N_1 = 1$, $N_2 = 2$, $N_3 = 3$. It follows from Eq. (5.3) that the concatenation of any realization of $\mathscr{W}_{L-1}$ with any realization of $\mathscr{W}_{L-2}$ yields two realizations of $\mathscr{W}_L$. The $2N_{L-1}N_{L-2}$ realizations of $\mathscr{W}_L$ thus obtained are not all different. Indeed, those of the form $\mathscr{W}_L = \mathscr{W}_{L-2}\mathscr{W}_{L-3}\mathscr{W}'_{L-2}$ are generated twice. This simple observation yields the recursion relation

$$N_L = N_{L-2}(2N_{L-1} - N_{L-2}N_{L-3}) \tag{5.4}$$

This equation is solved by defining the ratios $R_L = N_L/(N_{L-1}N_{L-2})$, which obey $R_L = 2 - 1/R_{L-1}$. The initial value $R_2 = 2$ readily yields $R_L = L/(L-1)$. The structural entropy of $\mathscr{W}_L$, defined through

$$S_L = \ln N_L \tag{5.5}$$

then obeys the recursion formula

$$S_L = S_{L-1} + S_{L-2} + \ln R_L \tag{5.6}$$

The solution of this last equation which assumes the initial values $S_0 = S_1 = 0$ reads

$$S_L = \sum_{M=2}^{L} F_{L+1-M} \ln R_M \tag{5.7}$$

The entropy per letter $S_{\text{Fib}} = \lim_{L\to\infty} S_L/F_{L+1}$ of the random Fibonacci sequence is therefore given by

$$\begin{aligned} S_{\text{Fib}} &= \sum_{M\geqslant 2} \tau^{-M} \ln R_M \\ &= \sum_{M\geqslant 2} \tau^{-(M+2)} \ln M \\ &= 0.444399 \end{aligned} \tag{5.8}$$

We now build a random Fibonacci chain by putting atoms on a line, the bond lengths being in one-to-one correspondence with the letters of $\mathscr{W}$, according to the rule of Section 2. We define the Fourier amplitudes $\mathscr{G}_L(q)$ associated with the words $\mathscr{W}_L$ by a formula analogous to Eq. (2.11). Hence $\mathscr{G}_L(q)$ are random functions of q, for which we will derive statistical statements. Let us first notice that Eqs. (2.8)–(2.10) still hold for the random chain. From Eq. (5.3) there follows the random recursion relation

$$\mathscr{G}_L(q) = \begin{cases} \mathscr{G}_{L-1}(q) + e^{-iq\lambda_{L-1}}\mathscr{G}_{L-2}(q) & \text{(with prob } p\text{)} \\ \text{or} & \\ \mathscr{G}_{L-2}(q) + e^{-iq\lambda_{L-2}}\mathscr{G}_{L-1}(q) & \text{(with prob } r\text{)} \end{cases} \tag{5.9}$$

with the certain initial conditions $\mathscr{G}_0(q) = e^{-iq}$ and $\mathscr{G}_1(q) = e^{-iq(1+\xi)}$. It will turn out that it is sufficient for our purpose to consider the first two cumulants of the random Fourier amplitudes, namely

$$\begin{aligned} A_L(q) &= \langle \mathscr{G}_L(q) \rangle \\ B_L(q) &= \langle |\mathscr{G}_L(q)|^2 \rangle - |A_L(q)|^2 \end{aligned} \tag{5.10}$$

where the brackets imply averaging over all sources of randomness present in $\mathscr{W}_L$.

The following recursion relation for the averaged Fourier amplitudes $A_L(q)$ is easily derived form Eq. (5.9):

$$\begin{gathered} A_L(q) = (p + re^{-iq\lambda_{L-2}})\, A_{L-1}(q) + (r + pe^{-iq\lambda_{L-1}})\, A_{L-2}(q) \\ A_0(q) = e^{-iq}; \qquad A_1(q) = e^{-iq(1+\xi)} \end{gathered} \tag{5.11}$$

We have shown in Section 2 that the deterministic Fibonacci chain has delta peaks in its Fourier transform at a dense set of values of q, given by Eq. (2.14). The reason was that, for those values of the wavevector, the phases $\exp(-iq\lambda_{L-1})$ entering Eq. (2.12) go to unity, thus producing the largest possible growth of Fourier amplitudes. The very same mechanism holds for Eq. (5.11). Hence the averaged Fourier spectrum of the random Fibonacci chain has delta peaks at the same wavevectors as the deterministic chain.

Let us now turn to the second cumulants $B_L(q)$ of the Fourier amplitudes. It can be derived from Eq. (5.9) that these quantities obey the recursion

$$B_L(q) = B_{L-1}(q) + B_{L-2}(q) + 2pr\, \Delta_L(q)$$

with

$$\begin{aligned} \Delta_L(q) = {} & (1 - \cos q\lambda_{L-1})\, |A_{L-2}(q)|^2 + (1 - \cos q\lambda_{L-2})\, |A_{L-1}(q)|^2 \\ & - \mathrm{Re}\{(1 - e^{iq\lambda_{L-1}})(1 - e^{-iq\lambda_{L-2}})\, A^*_{L-1}(q)\, A_{L-2}(q)\} \end{aligned} \tag{5.12}$$

and with the initial conditions $B_0(q) = B_1(q) = 0$. The $\Delta_L(q)$ are smooth functions of q, and remain bounded as L goes to infinity, because the divergences of the averaged amplitudes $A_L(q)$ at values of q of the form (2.14) are exactly compensated by the vanishing of their prefactors in Eq. (5.12). Since the solution of this recursion reads

$$B_L(q) = 2pr \sum_{M=2}^{L} F_{L+1-M} \Delta_M(q) \tag{5.13}$$

the remarks made just above show that the quantity

$$\mathscr{S}(q) = \lim_{L \to \infty} \frac{B_L(q)}{F_{L+1}} = 2pr \sum_{M \geqslant 2} \tau^{-M} \Delta_M(q) \tag{5.14}$$

is a smooth, bounded function of q. The interpretation of our results is as follows.

(a) *For a resonant wavevector* of the form (2.14), $qa/2\pi = j + k\tau$, both $A_L(q)$ and $B_L(q)$ grow like F_{L+1}. Hence, the quantity $\mathscr{G}_L(q)/F_{L+1}$, having a finite average and a second cumulant of the order of $1/F_{L+1}$, is self-averaging in the limit of an infinite chain. Its certain complex limit value

$$\lim_{L \to \infty} \frac{\mathscr{G}_L(q)}{F_{L+1}} = \lim_{L \to \infty} \frac{A_L(q)}{F_{L+1}} = C_{jk} \tag{5.15}$$

is just the amplitude of the delta peak. C_{jk} has a smooth p dependence, being maximal in magnitude in the deterministic cases ($p = 0$ or 1).

(b) *For a generic wavevector*, namely a value of q which is neither of the form (2.14) nor too well approximated by those numbers, then $|A_L(q)|^2 \ll F_{L+1}$, in such a way that the quantity

$$\lim_{L \to \infty} \frac{\langle |\mathscr{G}_L(q)|^2 \rangle}{F_{L+1}} = \lim_{L \to \infty} \frac{B_L(q)}{F_{L+1}} = \mathscr{S}(q) \tag{5.16}$$

is identified by a standard argument with the density of the absolutely continuous part $\mathscr{S}(q)\, dq$ of the Fourier spectrum. This continuous component is entirely defined by Eq. (5.16), since the nongeneric values of q that we have excluded have clearly zero measure. We do not aim at being more rigorous on this point.

The random Fibonacci chain thus provides a tractable example of a random geometrical structure with a mixed Fourier spectrum.

5.2. The Random Penrose Tiling

We have shown in Section 4 how the matching rules could be relaxed in a deterministic fashion to produce a (right or left) chiral pattern which automatically yields a tiling of the plane and which even strictly respects the quasiperiodicity of the Penrose tiling.

Let us now define, in close analogy with the random Fibonacci sequence, the (locally) random Penrose tiling as follows. Starting first with a Q triangle, we cut it either to the right or to the left with equal probabilities (in the usual statistical sense that, among a large number of initial triangles, we cut half of them along each direction). This first cut produces a random object, denoted $\tilde{Q}_1$, which has two equiprobable realizations. Starting now with a P triangle, we also cut it either to the right or to the left with equal probabilities, thus producing an elementary P triangle and a larger Q triangle that we identify with $\tilde{Q}_1$. The whole object, denoted $\tilde{P}_1$, has four possible realizations, since its definition has involved two binary choices. The process can be iterated, according to

$$\tilde{Q}_n = \tilde{P}_{n-1}\tilde{Q}_{n-1} \tag{5.17}$$

$$\tilde{P}_n = \tilde{Q}_n\tilde{P}_{n-1} \tag{5.18}$$

with the convention that the initial data $\tilde{P}_0$, $\tilde{Q}_0$ are just elementary P and Q tiles. At the nth step of the random inflation, $\tilde{P}_n$ and $\tilde{Q}_n$ are made of the very same numbers of tiles as their deterministic counterparts considered above: their tiles are just reshuffled.

Let us now determine the structural entropy of the infinite random Penrose tiling, in analogy with the one-dimensional case. Let M_n and N_n denote the numbers of different realizations of $\tilde{Q}_n$ and $\tilde{P}_n$, respectively: $M_0 = N_0 = 1$, $M_1 = 2$, $N_1 = 4$. The random recursive procedure (5.17)–(5.18) generates twice the same realization of $\tilde{Q}_n$ or $\tilde{P}_n$ in some cases, described in a generic way on Fig. 7. Consider first the $\tilde{Q}_n$ triangle of Fig. 7a: this pattern is obtained either as $\tilde{Q}_n = (\tilde{Q}_{n-1}\tilde{P}_{n-2})\,\tilde{Q}'_{n-1}$ or as $\tilde{Q}_n = (\tilde{Q}'_{n-1}\tilde{P}_{n-2})\,\tilde{Q}_{n-1}$. This effect leads to the following equation:

$$M_n = 2M_{n-1}N_{n-1} - M_{n-1}^2 N_{n-2} \tag{5.19}$$

The $\tilde{P}_n$ triangle of Fig. 7b is also generated twice, namely either as $\tilde{P}_n = (\tilde{P}_{n-1}(\tilde{P}_{n-2}\tilde{Q}_{n-2}))(\tilde{Q}_{n-1}\tilde{P}'_{n-2})$ or as $\tilde{P}_n = (\tilde{P}_{n-1}(\tilde{P}'_{n-2}\tilde{Q}_{n-2}))(\tilde{Q}_{n-1}\tilde{P}_{n-2})$. Hence we have

$$N_n = 2M_n N_{n-1} - M_{n-1}M_{n-2}N_{n-1}N_{n-2}^2 \tag{5.20}$$

We then define the entropies

$$S_{2n+1} = \ln M_n; \qquad S_{2n+2} = \ln N_n \tag{5.21}$$

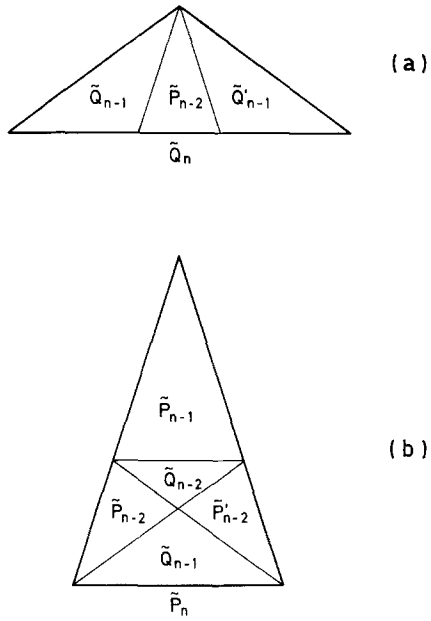

Fig. 7. Patterns that are generated twice in the cutting procedure (a) for $\tilde{Q}_n$, (b) for $\tilde{P}_n$.

These quantities obey the recursion equation

$$S_L = S_{L-1} + S_{L-2} + \ln R_L \tag{5.22}$$

which is identical to Eq. (5.6), with $S_1 = S_2 = 0$, and with the following definition of the ratios R_L:

$$R_{2n+1} = x_n = \frac{M_n}{M_{n-1} N_{n-1}}; \qquad R_{2n+2} = y_n = \frac{N_n}{M_n N_{n-1}} \tag{5.23}$$

These quantities are determined by the recursion relations

$$x_n = 2 - \frac{1}{y_{n-1}}; \qquad y_n = 2 - \frac{1}{x_n x_{n-1} y_{n-1}} \tag{5.24}$$

and the initial values $x_1 = y_1 = 2$. The recursions (5.24) is not soluble in a closed form. The entropy per tile of the random Penrose tiling

$$S_{\text{Pen}} = \lim_{n \to \infty} \frac{\ln M_n}{F_{2n+1}} = \lim_{n \to \infty} \frac{\ln N_n}{F_{2n+2}} = \lim_{L \to \infty} \frac{S_L}{F_L} \tag{5.25}$$

has the following expression, to be evaluated numerically:

$$S_{\text{Pen}} = \sum_{M \geqslant 3} \tau^{1-M} \ln R_M = 0.606094 \tag{5.26}$$

This value is larger than the entropy S_{Fib} of the random Fibonacci chain, and only slightly smaller than the entropy

$$S_{\text{mix}} = -(\tau^{-1} \ln \tau^{-1} + \tau^{-2} \ln \tau^{-2}) = 0.665018$$

of a random mixture of two types of objects with concentrations τ^{-1} and τ^{-2}.

Figure 8 shows one among the $N_6 = e^{S_{14}} \approx 1.2 \times 10^{99}$ different realizations of $\tilde{P}_6$, to be compared with the deterministic Penrose tiling P_6^{R} of Fig. 4 and the right chiral tiling P_6 of Fig. 6. These three patterns are made of the same numbers of tiles of each type.

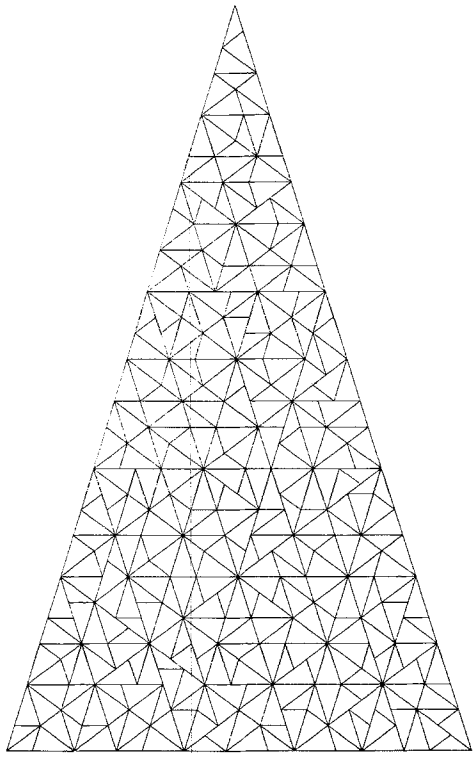

Fig. 8. A random Penrose tiling after six steps of the cutting procedure.

The study of the Fourier spectrum of the random Penrose tiling is fully analogous to that of the random Fibonacci chain, explained in detail in Section 5.1. The above definitions imply that the Fourier amplitudes $\tilde{P}_n(\mathbf{q})$, $\tilde{Q}_n(\mathbf{q})$ are random variables, which obey

$$\tilde{Q}_n(q) = \begin{cases} \exp(i\mathbf{q}\cdot\tau^n\hat{e}_3)[\tilde{P}_{n-1}(R^3\mathbf{q}) + \tilde{Q}_{n-1}(R^4\mathbf{q})] \\ \text{or} \\ \exp(-i\mathbf{q}\cdot\tau^n\hat{e}_0)\,\tilde{P}_{n-1}(R^7\mathbf{q}) + \exp(-i\mathbf{q}\cdot\tau^{n+1}\hat{e}_0)\,\tilde{Q}_{n-1}(R^6\mathbf{q}) \end{cases} \tag{5.27}$$

$$\tilde{P}_n(q) = \begin{cases} \exp(-i\mathbf{q}\cdot\tau^{n-1}\hat{e}_1)\,\tilde{P}_{n-1}(R^3\mathbf{q}) + \exp(-i\mathbf{q}\cdot\tau^n\hat{e}_0)\,\tilde{Q}_n(R^7\mathbf{q}) \\ \text{or} \\ \exp(-i\mathbf{q}\cdot\tau^n\hat{e}_0)\,\tilde{P}_{n-1}(R^7\mathbf{q}) + \exp(-i\mathbf{q}\cdot\tau^{n+1}\hat{e}_1)\,\tilde{Q}_{n-1}(R^3\mathbf{q}) \end{cases} \tag{5.28}$$

The initial values $\tilde{P}_0(\mathbf{q})$, $\tilde{Q}_0(\mathbf{q})$ are certain (nonrandom) quantities, equal to the Fourier transforms of the given mass distributions of both types of tiles. Both alternatives of the rhs of Eqs. (5.27) and (5.28) are taken with equal probabilities, and this source of randomness is independent of those already present in the amplitudes that are added. Since Eqs. (5.27) and (5.28) have the very same structure as Eq. (5.9), the way to solve them follows the same lines, although the notation is much lengthier. The averaged Fourier amplitudes

$$\bar{P}_n(\mathbf{q}) = \langle \tilde{P}_n(\mathbf{q}) \rangle; \qquad \bar{Q}_n(\mathbf{q}) = \langle \tilde{Q}_n(\mathbf{q}) \rangle \tag{5.29}$$

obey two coupled linear recursion relations that are very easily derived from Eqs. (5.27) and (5.28). These equations are analogous to Eq. (5.11): they imply that the averaged amplitudes have delta peaks for the same wavevectors of the form (3.34) as the deterministic Penrose tiling. The study of the second cumulants of the random amplitudes is more intricate. In order to obtain a closed set of equations analogous to Eq. (5.12), one has to consider four times ten sequences of cumulants $B_{n,k}^{(j)}$, namely

$$\begin{aligned} B_{n,k}^{(1)}(\mathbf{q}) &= \langle \tilde{P}_n(\mathbf{q})\, \tilde{P}_n^*(R^k\mathbf{q}) \rangle_c \\ B_{n,k}^{(2)}(\mathbf{q}) &= \langle \tilde{P}_n(\mathbf{q})\, \tilde{Q}_n^*(R^k\mathbf{q}) \rangle_c \\ B_{n,k}^{(3)}(\mathbf{q}) &= \langle \tilde{Q}_n(\mathbf{q})\, \tilde{Q}_n^*(R^k\mathbf{q}) \rangle_c \\ B_{n,k}^{(4)}(\mathbf{q}) &= \langle \tilde{P}_{n-1}(\mathbf{q})\, \tilde{Q}_n^*(R^k\mathbf{q}) \rangle_c \end{aligned} \tag{5.30}$$

for $0 \leqslant k \leqslant 9$; the subscript $\langle \cdot \rangle_c$ means that the product of averages has to be subtracted from the averaged product. It can be shown that the $B_{n,k}^{(j)}$ obey inhomogeneous recursion relations analogous to Eq. (5.12). This set of equations connects different values of j and k; their source terms, which generalize the $\Delta_L(q)$ of Eq. (5.12), are quadratic in the averaged amplitudes

(5.29). The smoothness of these source terms ensures the existence of an absolutely continuous part in the Fourier spectrum, with a density

$$\mathscr{S}(\mathbf{q}) = \lim_{n \to \infty} \frac{B_{n,0}^{(1)}(\mathbf{q})}{F_{2n+2}} = \lim_{n \to \infty} \frac{B_{n,0}^{(3)}(\mathbf{q})}{F_{2n+1}} \tag{5.31}$$

which is tenfold rotationally symmetric, i.e., $\mathscr{S}(\mathbf{q}) = \mathscr{S}(R^k \mathbf{q})$ for $0 \leqslant k \leqslant 9$.

Thus the random Penrose lattice, just like the random Fibonacci chain, has a mixed Fourier spectrum. There is enough randomness to yield both an extensive entropy and an absolutely continuous part in the Fourier spectrum, but there remains a partial perfect long-range translational order, attested by the presence of delta peaks.

6. FURTHER GENERALIZATIONS AND DISCUSSION

We have shown how generalized inflation rules can produce new tilings of the plane, made of Robinson triangles, which violate Penrose's celebrated matching rules. Although these tilings have infinitely many new kinds of patterns with respect to Penrose tilings, the most obvious one being three bond lengths, they have (at least partially) a quasiperiodic diffraction spectrum.

The chiral tilings introduced in Section 4 have a strictly quasiperiodic tenfold symmetric Fourier spectrum. A much larger class of deterministic tilings sharing that property can be built using the same idea. Indeed, any set of generalized inflation rules which is uniform in space at a given generation and either is independent of the generation label n or depends on n in a periodic way can be studied along the lines of Section 4. Two simple examples of such rules are as follows: (a) Cut all P triangles to the right and all Q triangles to the left. (b) Cut all triangles to the right if n is even, to the left if n is odd.

The (locally) random tilings of Section 5 have both an extensive structural entropy and a mixed Fourier spectrum, made of two parts, namely the same dense set of delta peaks as the Penrose tiling, with smaller intensities, and a smooth (absolutely continuous) component. Hence, apart from their obvious perfect rotational order (the tiles only have ten discrete possible orientations), the random tilings have a partial but perfect long-range translational order. The class of tilings with a mixed spectrum that can be described by our approach is also quite large. It includes in particular the globally random tilings, defined as follows. The cutting rules are chosen at random at each generation (e.g., one binary choice to cut the P's to the right or to the left, and another binary choice for the Q's, or the

same choice for both types of tiles), but hold identically for all triangles at a given generation. The entropy of such a construction is therefore proportional to the generation label n; it grows only like the logarithm of the number of tiles. The Fourier spectrum of globally random tilings can also be studied by the approach developed in Section 5. The only difference is that the amplitudes of parts of the tiling which are added up in random recursion relations, such as (5.9) and (5.27) and (5.28), are now correlated variables. Hence, the number of cumulants needed to get a closed set of equations is higher than in Section 5, but still finite, and the qualitative results remain the same: both locally and globally random tilings have a mixed Fourier spectrum.

The above study of tilings generated by locally random inflation rules may be relevant to generic random tilings, obtained by putting together P and Q tiles without obeying the matching rules. As mentioned in Section 4, the requirement of tiling a part of the plane without overlaps or holes is a strong nonlocal constraint on such tile arrangements, thus making the tiling problem very difficult. The structural entropy S_{til} of this model is certainly slightly larger than the entropy $S_{\text{Pen}} = 0.606$ of the subclass of random tilings that we have described. Besides the actual value of S_{til}, a question of more physical relevance remains open, namely the nature of the Fourier spectrum of these generic random tilings. There is a simple example of a random tiling with a mixed Fourier transform, namely stringing two types of segments, with commensurable lengths such as l and $2l$, at random on a line.

In closer connection with some previous work quoted in the introduction, we can also characterize the tilings produced by generalized inflation rules by looking at their extension in "perpendicular space." This notion shows up in a natural way when generating quasiperiodic tilings by the projection method. Let A and B be any two points of one of our tilings, either deterministic or random, after n steps of the inflation procedure. The vector $\mathbf{AB}$ can be shown, by induction on n, to be a linear combination, with integer coefficients, of the five unit vectors $\hat{e}_k$:

$$\mathbf{AB} = \sum_{k=0}^{4} N_k \hat{e}_k \tag{6.1}$$

The components N_k are unique, up to the addition of an integer to all of them, since $\sum_{k=0}^{4} \hat{e}_k = 0$. Hence $\mathbf{AB}$ can be viewed as the projection onto the tiling plane (E) of the five-dimensional vector

$$\mathbf{AB}^{(5)} = \sum_{k=0}^{4} N_k \hat{e}_k^{(5)} \tag{6.2}$$

where $\hat{e}_k^{(5)}$ form an orthonormal basis in Euclidean five-dimensional space $\mathbb{R}^5$. The ambiguity on the N_k is such that $\mathbf{AB}^{(5)}$ is only defined by Eq. (6.2) up to a translation by the diagonal vector $\Delta^{(5)} = \sum_{k=0}^{4} \hat{e}_k^{(5)}$. The sum of the tiling plane (E) and of the space generated by $\Delta^{(5)}$ has an orthogonal plane (two-dimensional subspace) $(E^\perp)$, hence called perpendicular space. The $\hat{e}_k^{(5)}$ project in that space onto five unit vectors $\hat{e}_k^\perp$. Coordinate axes can be chosen such that $\hat{e}_k^\perp$ makes the angle $k \cdot 4\pi/5$ with the x axis: in rough words, the unit vectors rotate twice faster in $(E^\perp)$ than they do in (E), the plane of the tiling. The projection of $\mathbf{AB}^{(5)}$ onto $(E^\perp)$ reads

$$\mathbf{AB}^\perp = \sum_{k=0}^{4} N_k \hat{e}_k^\perp \tag{6.3}$$

This expression is free of the above ambiguity, since $\sum_{k=0}^{4} \hat{e}_k^\perp = 0$, as it should, since $\Delta^{(5)}$ and $(E^\perp)$ are orthogonal. To summarize, to any vector (6.1) joining two tiling vertices, we can associate a unique vector (6.3) in perpendicular space. Thus we can build an image of our tilings in $(E^\perp)$, up to an irrelevant global translation and rotation. Let (A, B, C) and (D, E, F) denote the corners of the triangles P_n and Q_n, as in Fig. 1, at the nth generation. For these particular points, Eq. (6.1) reads

$$\begin{aligned}
\mathbf{AB} &= -F_{n+1}\hat{e}_1 - F_n(\hat{e}_0 + \hat{e}_2) \\
\mathbf{AC} &= F_{n+1}\hat{e}_4 + F_n(\hat{e}_0 + \hat{e}_3) \\
\mathbf{DE} &= F_n\hat{e}_3 + F_{n-1}(\hat{e}_2 + \hat{e}_4) \\
\mathbf{DF} &= -F_n\hat{e}_2 - F_{n-1}(\hat{e}_1 + \hat{e}_3)
\end{aligned} \tag{6.4}$$

It is then easy, using the definitions of $\hat{e}_k$ and $\hat{e}_k^\perp$ and the identities (2.6), to compute the following vector norms (distances):

$$AB = AC = EF = \tau^n; \qquad BC = DE = DF = \tau^{n-1} \tag{6.5}$$

$$AB^\perp = AC^\perp = EF^\perp = \tau^{-n}; \qquad BC^\perp = DE^\perp = DF^\perp = \tau^{-(n-1)} \tag{6.6}$$

While Eq. (6.5) just expresses that P_n and Q_n are τ^n times larger than the elementary tiles P_0 and Q_0, Eq. (6.6) show that all these distances shrink to zero in perpendicular space. Since, at each generation n, any new vertex can be joined to one of the tiling corners by a sum of at most three vectors of the form (6.4), we conclude readily that the tilings produced by our generalized inflation rules, either deterministic or random, have an extension (diameter) in perpendicular space which stays finite in the limit of an infinite sample.

To conclude, let us summarize the main points of this article. We have studied here the interplay between two properties of tilings (made of

Robinson triangles): their inflation (substitution) properties and their Fourier spectra. This study shows that quasiperiodicity is robust (in an intuitive sense) to changes in the rules for tiling the plane. It shows also that the constraint of the existence of inflation rules is strong: in particular, the "width" in perpendicular space of the strip which would generate the tiling is finite. We should also mention that one of our motivations in this work was to try to find a two-dimensional analogue of the structure we studied in one dimension,[14,15] which gave rise to a singular continuous Fourier spectrum. Instead of giving such a spectrum, the structures studied here have in general a mixed spectrum, i.e., they contain an absolutely continuous part as well as a discrete one.

ACKNOWLEDGMENTS

Part of this work was done during visits of J.M.L. to the Universities of Oxford and Edinburgh, supported by the French–British Prize. C. G. thanks M. Duneau, A. Katz, C. Oguey, A. Pavlovitch, and M. Ronchetti for interesting discussions about the Penrose tiling.

REFERENCES

1. P. J. Steinhardt and S. Ostlund, *The Physics of Quasicrystals* (World Scientific, Singapore, 1987).
2. T. C. Lubensky, J. E. S. Socolar, P. J. Steinhardt, P. A. Bancel, and P. A. Heiney, *Phys. Rev. Lett.* **57**:1440 (1986).
3. M. Kléman and A. Pavlovitch, *J. Phys.* (Paris) **C3**:229 (1986).
4. D. Shechtman and I. Blech, *Metall. Trans.* **16A**:1005 (1985).
5. P. W. Stephens and A. I. Goldman, *Phys. Rev. Lett.* **56**:1168 (1986); Errata, *Phys. Rev. Lett.* **57**:2331 (1986).
6. P. M. Horn, W. Malzfeldt, D. P. DiVincenzo, J. Toner, and R. Gambino, *Phys. Rev. Lett.* **57**:1444 (1986).
7. V. Elser, in *Proceedings of the XVth International Colloquium on Group Theoretical Methods in Physics* (World Scientific, Singapore, 1987), pp. 162–183.
8. B. Minchau, K. Y. Szeto, and J. Villain, *Phys. Rev. Lett.* **58**:1960 (1987).
9. M. Perreau and J. C. S. Lévy, University Paris VII, preprint (1988).
10. C. Henley, *J. Phys. A* **21**:1649 (1988).
11. S. Aubry and C. Godrèche, *J. Phys.* (Paris) **C3**:187 (1986).
12. S. Aubry, C. Godrèche, and F. Vallet, *J. Phys.* (Paris) **48**:327 (1987).
13. C. Godrèche, J. M. Luck, and F. Vallet, *J. Phys. A* **20**:4483 (1987).
14. S. Aubry, C. Godrèche, and J. M. Luck, *Europhys. Lett.* **4**:639 (1987).
15. S. Aubry, C. Godrèche, and J. M. Luck, *J. Stat. Phys.* **51**:1033 (1988).
16. R. M. Robinson, University of California, preprint (1975).
17. B. Grünbaum and G. C. Shephard, *Tilings and Patterns* (Freeman, New York, 1987), Chapter 10.
18. C. Godrèche and H. Orland, *J. Phys.* (Paris) **C3**:197 (1986).
19. E. Bombieri and J. E. Taylor, *J. Phys.* (Paris) **C3**:19 (1986); *Contemp. Math.* **64**:241 (1987).